J|A|C|S
ARTICLES
Published on Web 10/15/2002

[Ni^{0}L]-Catalyzed Cyclodimerization of 1,3-Butadiene: A Density Functional Investigation of the Influence of Electronic and Steric Factors on the Regulation of the Selectivity

Sven Tobisch*,† and Tom Ziegler‡

Contribution from the Institut für Anorganische Chemie der Martin-Luther-Universität Halle-Wittenberg, Fachbereich Chemie, Kurt-Mothes-Strasse 2, D-06120 Halle, Germany, and Department of Chemistry, University of Calgary, University Drive 2500, Calgary, Alberta, Canada T2N 1N4

Received March 22, 2002. Revised Manuscript Received June 3, 2002

Abstract: We present a comprehensive theoretical investigation of the influence of the ligand L on the regulation of the product selectivity for the [Ni^{0}L]-catalyzed cyclodimerization of 1,3-butadiene. The investigation was based on density functional theory (DFT) and a combined DFT and molecular mechanics (QM/MM) approach for the real [bis(butadiene)Ni^{0}L] catalysts with L = PMe_3, **I**; PPh_3, **II**; P(^{i}Pr)$_3$, **III**; and $P(OPh)_3$, **IV**. The role of electronic and steric effects has been elucidated for all crucial elementary steps of the entire catalytic cycle. Allylic isomerization, allylic enantioface conversion, as well as oxidative coupling are shown to be influenced to a minor extent by electronic and steric effects. In contrast, the ligand's properties have a distinct influence on the preestablished equilibrium between the $\eta^3,\eta^1(C^1)$ and bis-η^3 forms **2** and **4**, respectively, of the [(octadienediyl)Ni^{II}L] complex and on the rate-determining reductive elimination following competing routes for generation of either VCH, *cis*-1,2-DVCB, or *cis*,*cis*-COD. Electronic factors are shown to predominantly determine the position of the kinetically mobile **2** ⇌ **4** equilibrium. **4** is the prevailing species for ligands L that are π-acceptors (L = $P(OPh)_3$) or weak σ-donors (L = PPh_3), while stronger σ-donors (L = PMe_3, P(^{i}Pr)$_3$) displace the equilibrium to the left. Steric bulk on the ligand as well as its π-acceptor ability act to facilitate the reductive elimination, while σ-donor abilities serve to retard this process. Electronic and steric factors are found to not influence uniformly the reductive elimination routes with either **2** or **4** involved. The regulation of the product selectivity is elucidated on the basis of both thermodynamic and kinetic considerations.

Introduction

The catalytic cyclodimerization of 1,3-dienes mediated by transition metal complexes is one of the key processes in homogeneous catalysis.[1] Ligand-stabilized zerovalent nickel [Ni^{0}L] complexes, in particular, have been shown as the most versatile and useful catalysts.[2] The stereoselective [Ni^{0}L]-catalyzed cyclodimerization of butadiene was the subject of comprehensive and systematic investigations by Wilke and co-workers and represents probably the most thoroughly examined reaction in homogeneous catalysis.[2,3]

This process gives rise to three major C_8-cyclohydrocarbons, namely *cis*,*cis*-cycloocta-1,5-diene (*cis*,*cis*-COD), *cis*-1,2-divinylcyclobutane (*cis*-1,2-DVCB), and 4-vinylcyclohex-1-ene (VCH).[4] As one of their important achievements, Wilke et al. demonstrated here for the first time that the composition of the cyclodimer products could be regulated by the properties of the ligand L, which nowadays is called "ligand tailoring". A detailed experimental investigation of the ligand influence on the product distribution in the [Ni^{0}L]-catalyzed cyclooligomerization of 1,3-butadiene was undertaken.[5] Heimbach et al.[5] have used a regression analysis of the cyclodimer product composition as a function of the steric (Tolman's cone angle θ)[6] and electronic (Tolman's χ parameter)[6] properties of a representative set of ligands L to concluded that the selectivity of the cyclodimerization is entirely determined by electronic factors.[5b,c] Although

* To whom correspondence should be addressed. E-mail: tobisch@chemie.uni-halle.de.
† Martin-Luther-Universität Halle-Wittenberg.
‡ University of Calgary.

(1) (a) Jolly, P. W.; Wilke, G. The Oligomerization and Co-oligomerization of Butadiene and Substituted 1,3-Dienes. In *The Organic Chemistry of Nickel, Vol. 2, Organic Synthesis*; Academic Press: New York, 1975; pp 133−212. (b) Jolly, P. W. Nickel-Catalyzed Oligomerization of 1,3-Dienes Related Reactions. In *Comprehensive Organometallic Chemistry*; Wilkinson, G., Stone, F. G. A., Abel, E. W., Eds.; Pergamon: New York, 1982; Vol. 8, pp 671−711.

(2) (a) Wilke, G. *Angew. Chem., Int. Ed. Engl.* **1963**, *2*, 105. (b) Wilke, G. *Angew. Chem., Int. Ed. Engl.* **1988**, *27*, 185. (c) Wilke, G.; Eckerle, A. Cyclooligomerizations and Cyclo-Co-Oligomerizations of 1,3-Dienes. In *Applied Homogeneous Catalysis with Organometallic Complexes*; Cornils, B., Herrmann, W. A., Eds.; VCH: Weinheim, Germany, 1996; pp 358−373.

(3) (a) Wilke, G. *Pure Appl. Chem.* **1978**, *50*, 677. (b) Wilke, G. *J. Organomet. Chem.* **1980**, *200*, 349.

(4) A fourth cyclodimer of butadiene, the 1-methylene-2-vinylcyclopentane (MVCP), is formed in the presence of secondary alcohols. This reaction, however, is not investigated in the present study.

(5) (a) Heimbach, P.; Kluth, J.; Schenkluhn, H.; Weimann, B. *Angew. Chem., Int. Ed. Engl.* **1980**, *19*, 569. (b) Heimbach, P.; Kluth, J.; Schenkluhn, H.; Weimann, B. *Angew. Chem., Int. Ed. Engl.* **1980**, *19*, 570. (c) Kluth, J. Ph.D. Thesis, University of Essen-Gesamthochschule, 1980.

(6) (a) Tolman, C. A. *J. Am. Chem. Soc.* **1970**, *92*, 2953. (b) Tolman, C. A. *Chem. Rev.* **1977**, *77*, 313.

10.1021/ja020423w CCC: $22.00

Scheme 1. Catalytic Cycle of the [Ni^{0}L]-catalyzed Cyclodimerization of Butadiene Consisting of the Most Feasible Pathway for Each of the Critical Elementary Reaction Steps[a]

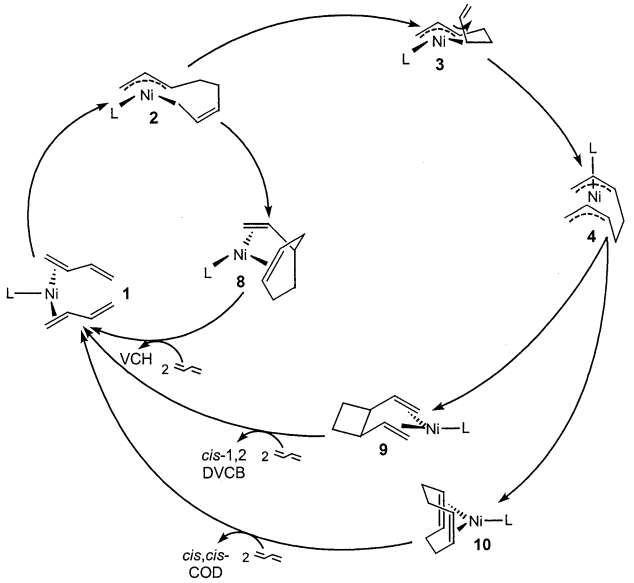

[a] For a detailed theoretical examination, see ref 7.

these studies provided a principal understanding of the ligand influence on the overall process, a detailed investigation of the influence of electronic and steric effects on the thermodynamic and kinetic aspects of each critical elementary step of the entire catalytic cycle is required for a deep, fundamental understanding of the factors that are decisive for the regulation of the cyclodimer formation's selectivity.

In our previous investigation we have theoretically explored the detailed mechanism of the [Ni^{0}L]-catalyzed cyclodimerization of 1,3-butadiene for the generic [bis(butadiene)Ni^{0}PH$_3$] catalyst.[7] This has let us predict the most feasible pathway for each of the critical elementary processes, identify the overall rate-determining step, and clarify what role η^3-allylic and η^1-allylic species actually play in the catalytic cycle. The present investigation is aimed at enhancing the mechanistic insight further by elucidating the role of electronic and steric factors for individual elementary steps. This allows us to contribute to the rationalization of the experimental results and to provide a deeper understanding of both the thermodynamic and the kinetic aspects of the regulation of the product selectivity in the [Ni^{0}L]-catalyzed cyclodimerization of 1,3-butadiene.

Catalytic Reaction Cycle. On the basis of the original proposal by Wilke et al.,[2,8] we have theoretically scrutinized in our previous investigation[7] all critical elementary steps of the entire catalytic cycle for the [Ni^{0}L]-catalyzed cyclodimerization of 1,3-butadiene with the generic [bis(butadiene)Ni^{0}PH$_3$] complex as model catalyst. Our investigation let us suggest the catalytic cycle shown in Scheme 1 for the multistep addition−elimination process, in terms of the most feasible reaction route for each of the individual crucial elementary processes.[9] Starting from the [bis(η^2-butadiene)Ni^{0}L] active catalyst complex **1**, the two η^2-coordinated butadienes undergo oxidative coupling, giving rise to the [(octadienediyl)Ni^{II}L] complex via C−C bond formation between the terminal noncoordinated carbon on each of the butadiene moieties. The [(octadienediyl)Ni^{II}L] complex is the crucial species of the catalytic cycle and it exists in several configurations, namely, the $\eta^3,\eta^1(C^1)$-allyl species **2**, the $\eta^3,\eta^1(C^3)$-allyl species **3**, and the bis(η^3-allyl) species **4**, all of which are in a preestablished equilibrium. Moreover, for **1** as well as for **2**−**4** there are several stereoisomeric forms (Figure 1) (vide infra). The species **2**, which is formed as the kinetic product of the oxidative coupling step, and **4** are the thermodynamically most stable isomers of the [(octadienediyl)Ni^{II}L] complex. The interconversion of various stereoisomeric forms of the [(octadienediyl)Ni^{II}L] complex via allylic syn−anti isomerization in **3** and allylic enantioface conversion in **2**, respectively, were found to be the most facile processes of the important steps involving the [(octadienediyl)Ni^{II}L] complex. The formation of the principal cyclodimer products proceeds via competing routes for reductive elimination starting from different [(η^3-octadienediyl)Ni^{II}L] species and giving rise to the [(η^4-cyclodimer)Ni^{0}L] products **8**, **9**, and **10**, respectively. The cyclodimers are liberated in a subsequent substitution with butadiene that regenerates **1**. **4** is the precursor for both the *cis*-1,2-DVCB and the *cis*,*cis*-COD generation paths along **4** → **9** and **4** → **10**, respectively, and VCH is formed along **2** → **8**. The reversibility of both the reductive elimination and the oxidative coupling has been demonstrated by experiment.[8,10] Bis(η^1-allyl) species are not involved in any viable pathways, either for isomerization or for reductive elimination, according to our previous investigation.[7]

Computational Models and Methods

Models. The entire catalytic cycle of the [Ni^{0}L]-catalyzed cyclodimerization of 1,3-butadiene consisting of the critical elementary steps displayed in Scheme 1, which are oxidative coupling of two butadienes, allylic syn−anti isomerization and allylic enantioface conversion, reductive elimination, and the equilibrium between the critical [(octadienediyl)Ni^{II}L] species **2** and **4**, was investigated for four real [bis(butadiene)Ni^{0}L] catalysts. The catalysts chosen contain ligands L with a broad range of electronic and steric properties through L = PMe_3, **I**; L = PPh_3, **II**; L = P(^{i}Pr)$_3$, **III**; and L = P(OPh)$_3$, **IV**. The regulation of the cyclodimer product selectivity is elucidated for these catalysts. In the examination of how electronic and steric factors influence the intrinsic kinetic barriers for oxidative coupling and reductive elimination as well as the equilibrium between **2** and **4**, the catalysts **V** with L = P(OMe)$_3$ and **VI** with L = P(^{t}Bu)$_3$ were considered as well in order to support further the conclusions drawn. We shall note here that the catalysts **V** and **VI** are known to redirect the cyclodimerization into a different reaction channel that predominantly yields cyclotrimer products.[2,5] The factors that are decisive in directing the [Ni^{0}L]-catalyzed butadiene cyclooligomerization into either the C_8- or the C_{12}-cyclohydrocarbon generating channel are, however, not considered in the present research and will be the subject of a forthcoming investigation.

To rationalize the electronic and steric properties of PR_3/P(OR)$_3$ ligands, several models have been proposed. The cone angle θ proposed by Tolman[6] is still one of the most popular concepts in coordination chemistry used to quantify the steric demand of the phosphine ligands. A theoretical approach based on molecular-mechanics calculations was proposed by Brown et al.[11] To describe the donor/acceptor ability of

(7) Tobisch, S.; Ziegler, T. *J. Am. Chem. Soc.* **2002**, *124*, 4881.
(8) Benn, R.; Büssemeier, B.; Holle, S.; Jolly, P. W.; Mynott, R.; Tkatchenko, I.; Wilke, G. *J. Organomet. Chem.* **1985**, *279*, 63.
(9) We have chosen the same numbers for key species participating in the catalytic cycle as in our previous investigation on the generic catalyst (ref 7) in order to ensure consistency in the presentation.
(10) (a) Heimbach, P.; Brenner, W. *Angew. Chem., Int. Ed. Engl.* **1967**, *6*, 800. (b) Jolly, P. W.; Tkatchenko, I.; Wilke, G. *Angew. Chem., Int. Ed. Engl.* **1971**, *10*, 329.

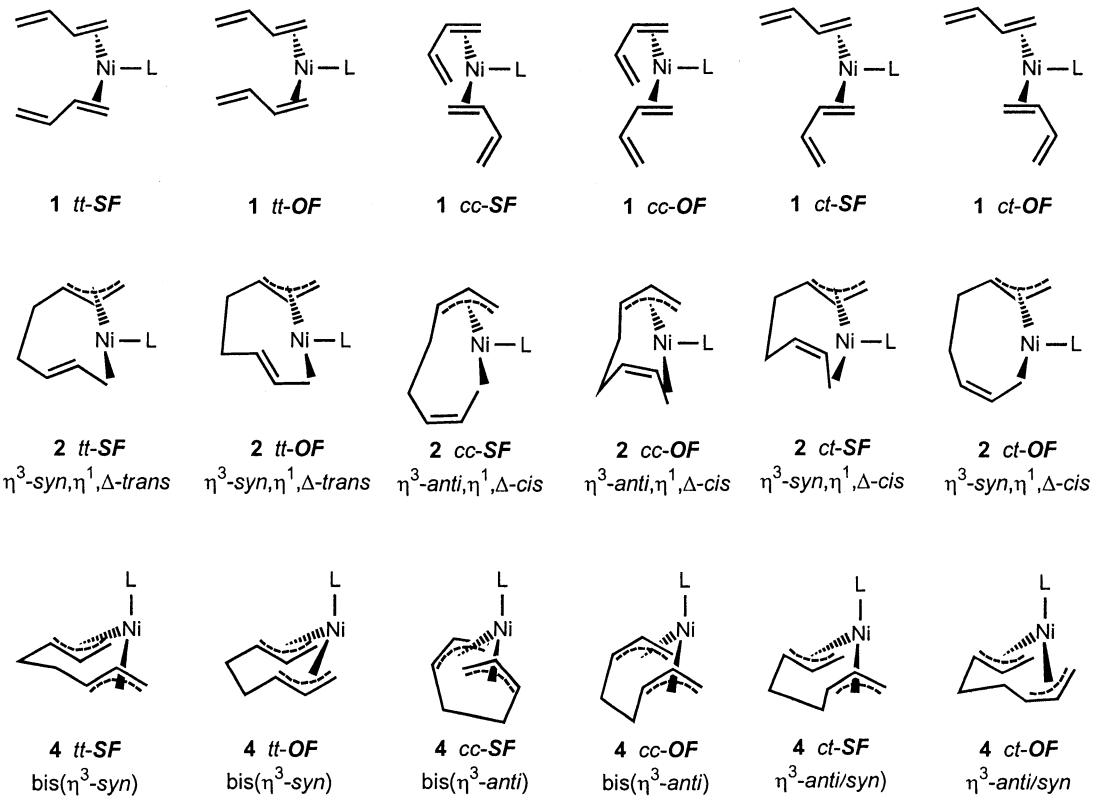

Figure 1. Stereoisomeric forms of the [bis(η^2-butadiene)Ni^{0}L] catalyst complex **1** and the related stereoisomers of the $\eta^3,\eta^1(C^1)$ species **2** and the bis-η^3 species **4** of the [(octadienediyl)Ni^{II}L] complex. SF and OF denotes the coordination of two *cis*-butadienes (*cc*) or of two *trans*-butadienes (*tt*) or of *cis*/*trans*-butadienes (*ct*) in **1** with the same or the opposite enantioface, respectively.

phosphine ligands, Tolman introduced the electronic parameter χ, which was based on the values of CO stretching frequencies in $Ni(CO)_3PR_3$ complexes.[6] Two alternative models for rationalizing the σ-donor and π-acceptor strengths of phosphines have been proposed by Drago[12] and Giering et al.[13] It was shown that the parameters used by Drago are linear combinations of the parameters used by the QALE method introduced by Giering et al.[14] In recent theoretical investigations[15] it was demonstrated that the energy of the lone pair at phosphorus, which is E_{HOMO} in free phosphines, correlates with experimental proton affinities, a parameter that has been employed widely to measure σ-basicity.[16] Therefore, lone-pair energies can serve as a measure of the σ-donor strength.[15] Furthermore, E_{LUMO} of the free phosphine was found to compare well with the back-donation component in $Fe(CO)_4PR_3$ complexes. Thus, E_{LUMO} can be used to estimate the π-acceptor strength.[15a] We shall note here that the correlation found for $E_{HOMO/LUMO}$ holds for a broad range of different ligands, with the only exception observed being PH_3. Accordingly, the σ-donor strength of the actual ligands investigated here should decrease in the following order, starting with the strongest σ-donor: $P(^tBu)_3 \sim P(^iPr)_3 > PMe_3 > PPh_3 > P(OMe)_3 \sim P(OPh)_3$. Moreover, the π-acceptor strength is likely to decrease in the following order: $P(OPh)_3 > P(OMe)_3 > PPh_3 > PMe_3 \sim P(^iPr)_3 \sim P(^tBu)_3$. According to the proposed cone angles θ, the steric demand decreases in the following order, starting from the most bulky ligand $P(^tBu)_3 > P(^iPr)_3 > PPh_3 > P(OPh)_3 > PMe_3 > P(OMe)_3$.

Methods. A 2-fold computational strategy was applied in order to gauge how the electronic and steric properties of individual ligands L influence crucial steps of the cyclodimerization process. The key stationary points along the most feasible pathways for all elementary steps in Scheme 1 were calculated by the pure DFT method, QM(DFT), as well as by a combined quantum mechanics/molecular mechanics method, QM/MM.

Density Functional Theory (DFT) Method. All reported DFT calculations were performed by using the TURBOMOLE program package developed by Ahlrichs et al.[17] The local exchange-correlation potential by Slater[18a,b] and Vosko et al.[18c] was augmented with gradient-corrected functionals for electron exchange according to Becke[18d] and correlation according to Perdew[18e] in a self-consistent fashion. This gradient-corrected density functional is usually termed BP86 in the literature. In recent benchmark computational studies, it was shown that the BP86 functional gives results in excellent agreement with the best wave function-based methods available today, for the class of reactions investigated here.[19]

For all atoms a standard all-electron basis set of triple-ζ quality for the valence electrons augmented with polarization functions was

(11) (a) Lee, K. J.; Brown, T. L. *Inorg. Chem.* **1992**, *31*, 289. (b) Choi, M.-G.; Brown, T. L. *Inorg. Chem.* **1993**, *32*, 5603.
(12) (a) Drago, R. S. *Organometallics* **1995**, *14*, 3408. (b) Drago, R. S.; Joerg, S. *J. Am. Chem. Soc.* **1996**, *118*, 2654.
(13) (a) Wilson, M. R.; Woska, D. C.; Prock, A.; Giering, W. P. *Organometallics* **1993**, *12*, 1742. (b) Woska, D.; Prock, A.; Giering, W. P. *Organometallics* **2000**, *19*, 4639.
(14) Fernandez, A.; Reyes, C.; Wilson, M. R.; Woska, D.; Prock, A.; Giering, W. P. *Organometallics* **1997**, *16*, 342.
(15) (a) Gonzalez-Banco, O.; Branchadell, V. *Organometallics* **1997**, *16*, 5556. (b) Senn, H. M.; Deubel, D. V.; Bloechl, P. E.; Togni, A.; Frenking, G. *J. Mol. Struct. (THEOCHEM)* **2000**, *506*, 233.
(16) (a) Jolly, C. A.; Chan, F.; Marynick, D. S. *Chem. Phys. Lett.* **1990**, *174*, 320. (b) Müller, B.; Reinhold, J. *Chem. Phys. Lett.* **1992**, *196*, 363. (c) Pacchioni, G.; Bagus, P. S. *Inorg. Chem.* **1992**, *31*, 4391. (d) Dias, P. B.; Minas de Piedade, M. E.; Martinho Simoes, J. A. *Coord. Chem. Rev.* **1994**, *135/136*, 737. (e) Howard, S. T.; Foreman, J. P.; Edwards, P. G. *Can. J. Chem.* **1997**, *75*, 60.
(17) (a) Häser, M.; Ahlrichs, R. *J. Comput. Chem.* **1989**, *10*, 104. (b) Ahlrichs, R.; Bär, M.; Häser, M.; Horn, H.; Kölmel, C. *Chem. Phys. Lett.* **1989**, *62*, 165.
(18) (a) Dirac, P. A. M. *Proc. Cambridge Philos. Soc.* **1930**, *26*, 376. (b) Slater, J. C. *Phys. Rev.* **1951**, *81*, 385. (c) Vosko, S. H.; Wilk, L.; Nussiar, M. *Can. J. Phys.* **1980**, *58*, 1200. (d) Becke, A. D. *Phys. Rev.* **1988**, *A38*, 3098. (e) Perdew, J. P. *Phys. Rev.* **1986**, *B33*, 8822.; *Phys. Rev. B* **1986**, *34*, 7406.
(19) (a) Bernardi, F.; Bottoni, A.; Calcinari, M.; Rossi, I.; Robb, M. A. *J. Phys. Chem.* **1997**, *101*, 6310. (b) Jensen, V. R.; Børve, K. *J. Comput. Chem.* **1998**, *19*, 947.

employed for the geometry optimization and the saddle-point search. The Wachters 14s/9p/5d set[20a] supplemented by two diffuse p[20a] and one diffuse d function[20b] contracted to (62111111/5111111/3111) was used for nickel, and standard TZVP basis sets[20c] were employed for phosphorus [a 13s/9p/1d set contracted to (73111/6111/1)], for carbon [a 10s/6p/1d set contracted to (7111/411/1)], and for hydrogen [a 5s/1p set contracted to (311/1)]. The frequency calculations were done by using standard DZVP basis sets,[20c] which consist of a 15s/9p/5d set contracted to (63321/531/41) for nickel, a 12s/8p/1d set contracted to (6321/521/1) for phosphorus, a 9s/5p/1d set contracted to (621/41/1) for carbon, and a 5s set contracted to (41) for hydrogen. The corresponding auxiliary basis sets were used for fitting the charge density.[20c,d]

Combined DFT and Molecular Mechanics (QM/MM) Approach. For the combined QM/MM calculations a modified version of the TURBOMOLE program package that includes the TINKER molecular mechanics program system[21] was used. The QM(DFT) and MM parts were coupled self-consistently according to the IMOMM method proposed by Maseras and Morokuma.[22] The QM part consisted of the generic [(C_8H_{12})NiPH_3] species in that the substituents on the phosphorus atom were replaced by hydrogen atoms. The alkyl and aryl groups attached to phosphorus for the actual PR_3/$P(OR)_3$ ligands were described by a MM3 molecular mechanics force field[23] without the electrostatic contributions. The fixed linked bond lengths were set to 0.438 Å for P—C_{sp^3}, to 0.478 Å for P—C_{sp^2}, and to 0.246 Å for P—O bonds. The UFF van der Waals parameter by Rappé et al. was used for the nickel atom,[24] whereas all other MM contributions involving the nickel atom were set to zero. The combined QM/MM methodology has successfully been applied for studying transition metal catalyzed reactions.[25]

Estimation of the Energetic Contribution of Electronic and Steric Factors. The combined QM/MM total energy can be defined as

$$E_{QM/MM} = E_{QM} + E_{QM-MM} + E_{MM} \quad (1)$$

where E_{QM} is the quantum mechanical energy of the QM part with the capping hydrogen atoms on the phosphorus included, that is, the generic [(C_8H_{12})NiPH_3] species in the present case. The term E_{MM} describes the molecular mechanics energy of the alkyl and aryl groups attached to phosphorus for the real ligands L (MM part), and E_{QM-MM} represents the nonbonded Coulombic and van der Waals interactions between the QM and MM parts, respectively. Taking the parent PH_3 ligand as the reference, the relative activation energies for an individual ligand L obtained at the QM level can be defined as

$$\Delta\Delta E^{\ddagger}(L) = \Delta E_{QM}{}^{\ddagger}(L) - \Delta E_{QM}{}^{\ddagger}(PH_3) \quad (2)$$

The contribution of steric factors to $\Delta\Delta E^{\ddagger}(L)$ can be estimated by the following relation

$$\Delta\Delta E_{st}{}^{\ddagger}(L) = \Delta E_{QM/MM}{}^{\ddagger}(L) - \Delta E_{QM}{}^{\ddagger}(PH_3) \quad (3)$$

since $\Delta E_{QM/MM}{}^{\ddagger}(L)$ can be considered to represent both the activation barrier for the generic species (with L = PH_3 treated electronically) and the steric effects of bulky substituents for the actual ligand L. We shall consider the remaining part of $\Delta\Delta E^{\ddagger}(L)$ to originate from electronic effects, which is estimated by the following relation

$$\Delta\Delta E_{el}{}^{\ddagger}(L) = \Delta\Delta E^{\ddagger}(L) - \Delta\Delta E_{st}{}^{\ddagger}(L) \quad (4)$$

This approach will also be applied to estimate electronic and steric contributions to thermodynamic reaction energies and to relative stabilities of different [(octadienediyl)Ni^{II}L] species such as **2** and **4** (section B).

Stationary Points. The geometry optimization and the saddle-point search were carried out by utilizing analytical/numerical gradients/Hessians according to standard algorithms for both QM(DFT) and QM/MM methodologies. No symmetry constraints were imposed in any case. The stationary points were identified exactly by the curvature of the potential-energy surface at these points corresponding to the eigenvalues of the Hessian. The reaction and activation enthalpies and free energies (ΔH, ΔG and $\Delta H^{\ddagger}$, $\Delta G^{\ddagger}$ at 298 K and 1 atm) were calculated at the pure DFT level of approximation for the most stable isomers of each of the key species of the entire catalytic reaction. For catalysts **II** (L = PPh_3) and **III** (L = $P(^iPr)_3$), the zero-point energy corrections (ZPC) and the thermal motion and entropy contributions calculated for catalyst **I** (L = PMe_3) were applied, while for **IV** (L = $P(OPh)_3$) the data calculated for **V** (L = $P(OMe)_3$) were used.

Labeling of the Molecules. Important species of the catalytic cycle were labeled with the arabic numbers given in Scheme 1.[9] The enantioface and the configuration (s-trans, s-cis) of the two prochiral butadiene moieties that are involved in the oxidative coupling are of crucial importance for the stereocontrol of the cyclodimer formation. The coupling can occur between two *cis*-butadienes (*cc*) or two *trans*-butadienes (*tt*) or between two butadienes of different configuration (*ct*) with either the same (denoted SF; i.e., same face) or the opposite (denoted OF; i.e., opposite face) enantioface of the two butadienes involved. This gives rise to several stereoisomers of **1**, which are schematically depicted in Figure 1, together with the related stereoisomers of the $\eta^3,\eta^1(C^1)$ and bis-η^3 octadienediyl species **2** and **4**, respectively. The several stereoisomeric pathways possible for each of the elementary steps were classified according to the kind of butadiene coupling to which the stereoisomeric form of the precursor corresponded.

Results and Discussion

We shall start our investigation by exploring each of the crucial elementary steps in Scheme 1 for the [bis(η^2-butadiene)-Ni^{0}L] catalyst **I**—**IV**, with L = PMe_3, PPh_3, $P(^iPr)_3$, and $P(OPh)_3$, respectively, at the pure QM(DFT) level of approximation. The complete collection of the results for different stereochemical pathways for each of the reaction steps is included in the Supporting Information (Tables S1—S6). In the discussion below, however, we will concentrate only on the most likely of the several stereochemical pathways for each process. It is interesting to note that the kinetic preference for an individual stereochemical pathway of a certain elementary process does not change upon variation of the catalyst.[26] The focus on this first part of our investigation is 2-fold: first, to evaluate whether the mechanistic conclusions drawn in our

(20) (a) Wachters, A. H. J. *J. Chem. Phys.* **1970**, *52*, 1033. (b) Hay, P. J. *J. Chem. Phys.* **1977**, *66*, 4377. (c) Godbout, N.; Salahub, D. R.; Andzelm, J.; Wimmer, E. *Can. J. Chem.* **1992**, *70*, 560. (d) TURBOMOLE basis set library.
(21) TINKER. Software Tools for Molecular Design, Version 3.6, 1998, developed by Prof. J. W. Ponder. Information about TINKER can be found at http://dasher.wustl.edu/tinker.
(22) Maseras, F.; Morokuma, K. *J. Comput. Chem.* **1995**, *16*, 1170.
(23) (a) Full MM3(96) parameter set including π-systems. (b) Allinger, N. L.; Yuh, Y. H.; Lii, J.-H. *J. Am. Chem. Soc.* **1989**, *111*, 8551. (c) Lii, J.-H.; Allinger, N. L. *J. Am. Chem. Soc.* **1989**, *111*, 8566. (d) Lii, J.-H.; Allinger, N. L. *J. Am. Chem. Soc.* **1989**, *111*, 8576. (e) Allinger, N. L.; Geise, H. J.; Pyckhout, W.; Paquette, L. A.; Gallucci, J. C. *J. Am. Chem. Soc.* **1989**, *111*, 1106. (f) Allinger, N. L.; Li, F.; Yan, L. *J. Comput. Chem.* **1990**, *11*, 848. (g) Allinger, N. L.; Li, F.; Yan, L.; Tai, J. C. *J. Comput. Chem.* **1990**, *11*, 868.
(24) Rappé, A. K.; Casewit, C. J.; Colwell, K. S.; Goddard, W. A., III; Skiff, W. M. *J. Am. Chem. Soc.* **1992**, *114*, 10024.
(25) (a) Deng, L.; Woo, T. K.; Cavallo, L.; Margl, P.; Ziegler, T. *J. Am. Chem. Soc.* **1997**, *119*, 6177. (b) Deng, L.; Ziegler, T.; Woo, T. K.; Margl, P.; Fan, L. *Organometallics* **1998**, *17*, 3240. (c) Deng, L.; Margl, P.; Ziegler, T. *J. Am. Chem. Soc.* **1999**, *121*, 6479. (d) Margl, P.; Deng, L.; Ziegler, T. *Organometallics* **1999**, *18*, 5701. (e) Matsubara, T.; Maseras, F.; Koga, N.; Morokuma, K. *J. Phys. Chem.* **1996**, *100*, 2573. (f) Musaev, D. G.; Froese, R. D. J.; Morokuma, K. *Organometallics* **1998**, *17*, 1850. (g) Vyboishchikov, S. F.; Musaev, D. G.; Froese, R. D. J.; Morokuma, K. *Organometallics* **2001**, *20*, 309. (h) Khoroshun, D. V.; Musaev, D. G.; Vreven, T.; Morokuma, K. *Organometallics* **2001**, *20*, 2007.

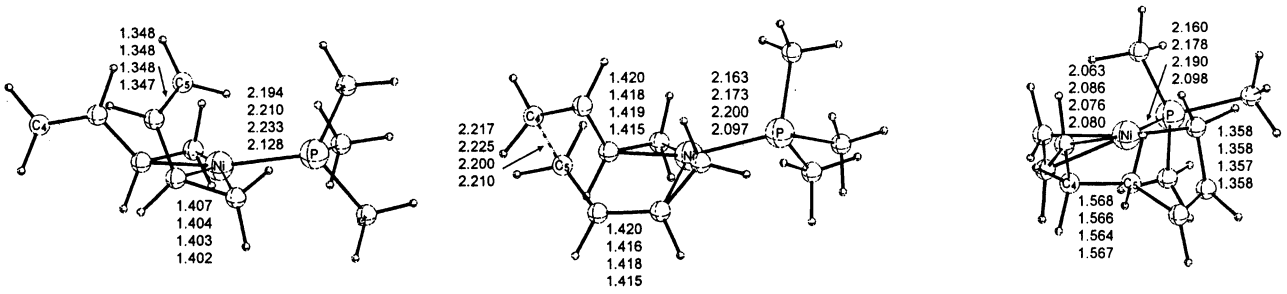

1 **TS[1-2]** **2**

Figure 2. Selected geometric parameters (Å) of the optimized structures of key species for oxidative coupling for the [bis(η^2-butadiene)Ni^{0}L] complex via the most feasible *ct*-OF stereochemical pathway along **1** → **2**. Values for individual degrees of freedom are given for L = PMe_3, **I**; PPh_3, **II**; $P(^iPr)_3$, **III**; $P(OPh)_3$, **IV**. Structures are displayed for **I**.

Table 1. Intrinsic Activation Enthalpies and Free Energies ($\Delta H_{int}^{\ddagger}/\Delta G_{int}^{\ddagger}$ in kcal mol^{-1}) and Reaction Enthalpies and Free Energies ($\Delta H_{int}/\Delta G_{int}$ in kcal mol^{-1}) for Oxidative Coupling for the [Bis(η^2-butadiene)Ni^{0}L] Complex via the Most Feasible *ct*-OF Stereochemical Pathway along **1** → **2**, Together with an Estimate of Electronic and Steric Contributions to Relative Activation Barriers and Reaction Energies ($\Delta\Delta E^{\ddagger}$, $\Delta\Delta E$ in kcal mol^{-1})[a-c]

	L = PH_3	**I**, L = PMe_3	**II**, L = PPh_3	**III**, L = $P(iPr)_3$	**IV**, L = $P(OPh)_3$	**V**, L = $P(OMe)_3$	**VI**, L = $P(tBu)_3$
$\Delta H_{QM}^{\ddagger}/\Delta G_{QM}^{\ddagger}$	6.97/9.91	6.79/9.30	7.30/9.81	7.13/9.64	7.25/9.88		
$\Delta H_{QM}/\Delta G_{QM}$	−6.65/−3.54	−7.38/−4.58	−6.40/−3.60	−7.41/−4.61	−6.84/−4.12		
$\Delta E_{QM}^{\ddagger}$	7.44	7.21	7.72	7.55	7.72	7.42	7.92
$\Delta E_{QM/MM}^{\ddagger}$		7.46	7.85	7.95	7.82	7.47	8.27
$\Delta\Delta E$ [b]		−0.23	0.28	0.11	0.28	−0.02	0.48
$\Delta\Delta E_{el}^{\ddagger}/\Delta\Delta E_{st}^{\ddagger}$		−0.25/0.02	−0.13/0.41	−0.40/0.51	−0.10/0.38	−0.05/0.03	−0.35/0.82
ΔE_{QM}	−8.12	−8.82	−7.84	−8.85	−8.32	−8.22	−10.86
$\Delta E_{QM/MM}$		−8.10	−8.07	−7.82	−7.97	−8.10	−8.97
$\Delta\Delta E$[c]		−0.70	0.28	−0.73	−0.20	−0.10	−2.74
$\Delta\Delta E_{el}/\Delta\Delta E_{st}$		−0.72/0.02	0.23/0.05	−1.03/0.30	−0.35/0.15	−0.12/0.02	−1.89/−0.85

[a] Intrinsic barriers and reaction energies relative to the [(η^2-*cis*/*trans*-butadiene)Ni^{0}L] OF isomer of **1**. The values for the generic catalyst taken from our previous study[7] are included for comparison. [b] $\Delta\Delta E^{\ddagger}$, the activation barrier relative to the parent PH_3 ligand, is calculated according to relation 2. The positive/negative sign indicates increased/decreased relative barrier. $\Delta\Delta E_{el}^{\ddagger}/\Delta\Delta E_{st}^{\ddagger}$, an estimate of electronic and steric contributions to the relative activation barrier $\Delta\Delta E^{\ddagger}$; is calculated according to relations 4 and 3, respectively. [c] $\Delta\Delta E$, the reaction energy relative to the parent PH_3 ligand, is calculated similarly to relation 2. The positive/negative sign indicates decreased/increased relative reaction energy. $\Delta\Delta E_{el}/\Delta\Delta E_{st}$, an estimate of electronic and steric contributions to the reaction energy $\Delta\Delta E$, is calculated similarly to relations 4 and 3, respectively.

previous investigation for the generic [bis(η^2-butadiene)Ni^0PH_3] catalyst are still valid or need to be reformulated upon variation of the catalyst and, second, to clarify the role of electronic and steric effects on the intrinsic barriers for oxidative coupling and reductive elimination and also on the equilibrium between the crucial [(octadienediyl)Ni^{II}L] species **2** and **4**. The subsequent part is devoted to elucidating the regulation of the selectivity of the cyclodimerization depending on the electronic and steric properties of L, with emphasis on both thermodynamic and kinetic aspects.

I. Exploration of the Influence of Electronic and Steric Factors for Crucial Elementary Steps. A. Oxidative Coupling. Commencing from the formal 16e$^-$ trigonal planar [bis(η^2-butadiene)Ni^{0}L] active catalyst complex **1**, oxidative coupling preferably takes place via formation of a C−C σ-bond between the terminal noncoordinated carbons C^4 and C^5 of the two η^2-butadiene moieties (Figure 2), which affords **2** as the kinetic product. The most feasible pathway occurs via OF-coupling of *cis*/*trans*-butadiene (Table S1), which also gives rise to the thermodynamically most stable stereoisomer of **2** in an overall thermoneutral process.

(26) For all catalyts investigated here we found the identical individual stereochemical pathway to be kinetically preferred for a certain elementary process as in our previous investigation of the generic [bis(butadiene)-Ni^0PH_3] catalyst (ref 7).

The geometry of the reacting butadienes in the transition states for the most feasible *ct*-OF pathway is seen to be very similar for all catalysts (Figure 2). TS[**1**−**2**] can be characterized as educt-like with a distance of ∼2.20−2.22 Å of the emerging C−C σ-bond. The intrinsic free activation barriers ($\Delta G_{int}^{\ddagger}$) along the most feasible *ct*-OF pathway (Table 1) are in a close interval of 9.3 kcal mol^{-1} (**I**, L = PMe_3) to 9.9 kcal mol^{-1} (**IV**, L = $P(OPh)_3$). The intrinsic reaction free energy (ΔG_{int}) exhibits a narrow range as well between −3.6 kcal mol^{-1} (**II**, L = PPh_3) and −4.6 kcal mol^{-1} (**III**, L = $P(^iPr)_3$).

Formally, oxidative coupling is accompanied by electron redistribution between the two [NiL] and [C_8H_{12}] moieties, such that the oxidation number of nickel increases by two (Ni^0 → Ni^{II}) during this process. Accordingly, σ-donor ligands are found to facilitate the oxidative coupling kinetically (cf. $\Delta\Delta E_{el}^{\ddagger}$ in Table 1), since they tend to alleviate the formal electron deficiency on nickel in TS[**1**−**2**] and therefore contribute to a lowering of the activation energy. Furthermore, electron-donating ligands act to stabilize **2** (section B) and, therefore, increasing σ-donor strength favors the process thermodynamically as well (cf. Table 1). With regards to the steric effect, it follows from the $\Delta\Delta E_{st}^{\ddagger}$ contribution that the oxidative coupling becomes retarded for ligands that are sterically bulky. This is understandable, since the steric interactions are likely to increase

Table 2. Thermodynamic Stabilities of the Most Stable Isomers of the **2** and **4** Species of the [(Octadienediyl)Ni^{II}L] Complex ($\Delta H/\Delta G$ in kcal mol^{-1}), Together with an Estimate of Electronic and Steric Contributions ($\Delta\Delta E_{el}/\Delta\Delta E_{st}$ in kcal mol^{-1})[a,b]

	L = PH_3	**I**, L = PMe_3	**II**, L = PPh_3	**III**, L = $P(^iPr)_3$	**IV**, L = $P(OPh)_3$	**V**, L = $P(OMe)_3$	**VI**, L = $P(^tBu)_3$
$\Delta H_{QM}/\Delta G_{QM}$[a]	−1.61/−0.97	0.07/0.50	−0.80/−0.37	2.88/3.31	−1.57/−1.06		
ΔE_{QM}	−1.11	0.64	−0.23	3.45	−1.10	−1.50	1.41
$\Delta E_{QM/MM}$		−1.10	−0.81	−0.48	−0.65	−1.08	−2.28
$\Delta\Delta E$[b]		1.75	0.88	4.56	0.01	−0.39	2.52
$\Delta\Delta E_{el}/\Delta\Delta E_{st}$		1.74/0.01	0.58/0.30	3.93/0.63	−0.45/0.46	−0.42/0.03	3.69/−1.17

[a] Difference in the thermodynamic stability between the bis(η^3-*syn*) *tt*-OF isomer of **4** and the η^3-*syn*,η^1(C^1),Δ-*cis* *ct*-OF isomer of **2** of the [(octadienediyl)Ni^{II}L] complex; the positive/negative sign indicates higher/lower stability of **2** relative to **4**. The values for the generic catalyst taken from our previous study[7] are included for comparison. [b] $\Delta\Delta E$, the thermodynamic stability relative to the parent PH_3 ligand, is calculated similarly to relation 2. $\Delta\Delta E_{el}/\Delta\Delta E_{st}$, an estimate of electronic and steric contributions to the reaction energy $\Delta\Delta E$, is calculated similarly to relations 4 and 3, respectively.

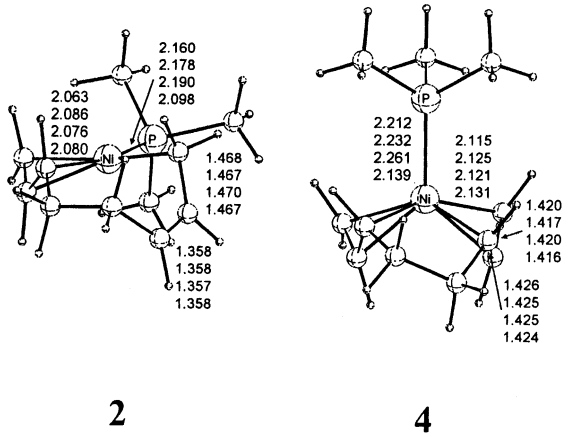

Figure 3. Selected geometric parameters (Å) of the optimized structures of the [(η^3-*syn*,η^1(C^1),Δ-*cis*-octadienediyl)Ni^{II}L] species **2** (*ct*-OF isomer) and of the [(bis(η^3-*syn*)-octadienediyl)Ni^{II}L] species **4** (*tt*-OF isomer) of the [(octadienediyl)Ni^{II}L] complex. See Figure 2.

during the process starting from the trigonal planar **1** and ending at **2**, where the ligand L resides in a square-planar conformation together with the η^3- and η^1(C^1)-allylic groups.

Thus, steric and electronic effects, which are seen to be small, are found to work in opposite directions and to some degree cancel. Consequently, the activation barriers are very similar for all catalysts, nearly independent of the actual ligand's nature. Overall, the oxidative coupling represents the one process (beside allylic isomerizations, section C) among all the crucial elementary steps that is least influenced by electronic and steric factors.

B. Equilibrium between the Crucial [(Octadienediyl)Ni^{II}L] Species 2 and 4. Among the different configurations of the crucial [(octadienediyl)Ni^{II}L] complex, which all are in a preestablished equilibrium, the η^3,η^1(C^1) species **2** and the bis-η^3 species **4** are prevailing. They represent the precursors for the final rate-determining reductive elimination step that affords the principal cyclodimer products along the three competing routes. The relative stabilities of **2** and **4** determine their actual thermodynamic population and play a crucial role in elucidating the thermodynamically related aspect of the selectivity of the cyclodimer formation.

In the examination of the ligand's influence on the **2** ⇌ **4** equilibrium, we shall focus on the most stable stereoisomer for each of them, namely the [(η^3-*syn*,η^1(C^1),Δ-*cis*-octadienediyl)-Ni^{II}L] *ct*-OF isomer of **2** and the [(bis(η^3-*syn*)-octadienediyl)-Ni^{II}L] *tt*-OF isomer of **4** (Figure 3). These stereoisomers have been unequivocally established as the most stable forms of **2** and **4**, respectively, both by NMR and by X-ray structural analysis.[8,27] A facile rearrangement of the initially generated **2** (which is the kinetic product of oxidative coupling) into **4** has been demonstrated in the stoichiometric cyclodimerization with PPh_3- and $P(OC_6H_4$-*o*-$Ph)_3$-stabilized complexes.[8]

The relative stabilities of **2** and **4** are known to be influenced by the ligand's properties. The bis-η^3 species **4** represents the energetically preferred mode of the Ni^{II}-bis(allyl-anion) coordination, since the formal negative charge is delocalized over the allylic moieties. In contrast, the η^3,η^1(C^1) coordination mode is energetically less favorable when compared with the bis-η^3 mode, since it requires the localization of the formal negative charge at one of the allylic groups on the terminal C^1 atom. The localization of the negative charge, however, can be supported by the presence of an electron-releasing ligand L. A detailed investigation of the ligand's influence on the preferred coordination mode in the [(octadienediyl)Ni^{II}L] complex has been undertaken by Jolly et al. by tracing the stoichiometric cyclodimerization with NMR.[8] For L = PCy_3, $P(^iPr)_3$, **2** was entirely detected, while for L = PPh_3, $P(OC_6H_4$-*o*-$Ph)_3$, **4** was confirmed as the thermodynamically favored species. A mixture of the **2** and **4** species was observed for the PMe_3-stabilized complex consisting predominantly of **2** (85%). This provides evidence that the equilibrium between **2** and **4** is shifted toward **2** with the increase of the σ-donor strength of L, whereas **4** becomes thermodynamically favored for weak σ-donors as well as for strong π-acceptor ligands.

The estimated contributions of electronic and steric factors to the relative stability between **2** and **4**, $\Delta\Delta E_{el}$ and $\Delta\Delta E_{st}$, respectively, in Table 2, follow a regular trend. Taking the generic PH_3 ligand as the reference, the increase in the ligand's donating ability correlates with the relative stabilization of **2** and is largest for the strong σ-donors $P(^iPr)_3$ and $P(^tBu)_3$. On the other hand, **4** becomes favored relative to **2** for π-acceptor ligands in the expected order $P(OPh)_3 > P(OMe)_3$. Moderate steric pressure introduced by the ligand is predicted to slightly favor **2** over **4** by ∼0.5 kcal mol^{-1}. Severe steric bulk, however, destabilizes the square-planar species **2** relative to the square-pyramidal species **4**, as observed for $P(^tBu)_3$.

Overall, the **2** ⇌ **4** equilibrium is found to be essentially determined by electronic factors, with sterics having a less pronounced influence. The calculated relative thermodynamic stabilities (ΔG) of **2** and **4** are in excellent agreement with experimental observations. For the strongest σ-donor $P(^iPr)_3$ as well as for the moderate σ-donor PMe_3 the [(octadienediyl)-Ni^{II}L] complex is predicted to exist predominantly in the

(27) (a) Brown, J. M.; Golding, B. T.; Smith, M. J. *Chem. Commun.* **1971**, 1240. (b) Barnett, B.; Büssemeier, B.; Heimbach, P.; Jolly, P. W.; Krüger, C.; Tkatchenko, I.; Wilke, G. *Tetrahedron Lett.* **1972**, 1457. (c) Büssemeier, B. Ph.D. Thesis, University of Bochum, 1973. (d) Jolly, P. W.; Mynott, R.; Salz, R. *J. Organomet. Chem.* **1980**, *184*, C49.

Table 3. Intrinsic Activation Enthalpies and Free Energies ($\Delta H_{int}^{\ddagger}/\Delta G_{int}^{\ddagger}$ in kcal mol^{-1}) and Reaction Enthalpies and Free Energies ($\Delta H_{int}/\Delta G_{int}$ in kcal mol^{-1}) for Reductive Elimination Affording VCH for the [(Octadienediyl)Ni^{II}L] Complex via the Most Feasible *cc*-SF Stereochemical Pathway along **2** → **8**, Together with an Estimate of Electronic and Steric Contributions to Relative Activation Barriers and Reaction Energies ($\Delta\Delta E^{\ddagger}$, $\Delta\Delta E$ in kcal mol^{-1})[a-c]

	L = PH_3	**I**, L = PMe_3	**II**, L = PPh_3	**III**, L = $P(^iPr)_3$	**IV**, L = $P(OPh)_3$	**V**, L = $P(OMe)_3$	**VI**, L = $P(^tBu)_3$
$\Delta H_{QM}^{\ddagger}/\Delta G_{QM}^{\ddagger}$	22.52/23.00	23.58/23.74	23.17/23.33	21.67/21.83	20.50/20.54		
$\Delta H_{QM}/\Delta G_{QM}$	−13.38/−12.48	−11.43/−11.18	−13.38/−12.71	−14.14/−13.48	−14.96/−14.24		
$\Delta E_{QM}^{\ddagger}$	23.45	24.56	24.15	22.65	21.50	22.25	17.41
$\Delta E_{QM/MM}^{\ddagger}$		23.43	23.20	21.54	22.54	23.40	16.57
$\Delta\Delta E^{\ddagger}$ [b]		1.11	0.70	−0.80	−1.95	−1.20	−6.04
$\Delta\Delta E_{el}^{\ddagger}/\Delta\Delta E_{st}^{\ddagger}$		1.13/−0.02	0.95/−0.25	1.11/−1.91	−1.04/−0.91	−1.15/−0.05	0.84/−6.88
ΔE_{QM}	−14.13	−12.58	−14.11	−14.87	−15.68	−14.65	−20.43
$\Delta E_{QM/MM}$		−14.16	−15.21	−16.05	−11.01	−14.20	−21.43
$\Delta\Delta E$ [c]		1.55	0.02	−0.74	−1.55	−0.52	−6.30
$\Delta\Delta E_{el}/\Delta\Delta E_{st}$		1.58/−0.03	1.10/−1.08	1.18/−1.92	−0.55/−1.00	−0.45/−0.07	1.00/−7.30

[a] Intrinsic barriers and reaction energies relative to the [(η^3-*anti*,η^1(C^1),Δ-*cis*-octadienediyl)Ni^{II}L] *cc*-OF isomer of **2**. The values for the generic catalyst taken from our previous study[7] are included for comparison. [b,c] See Table 1.

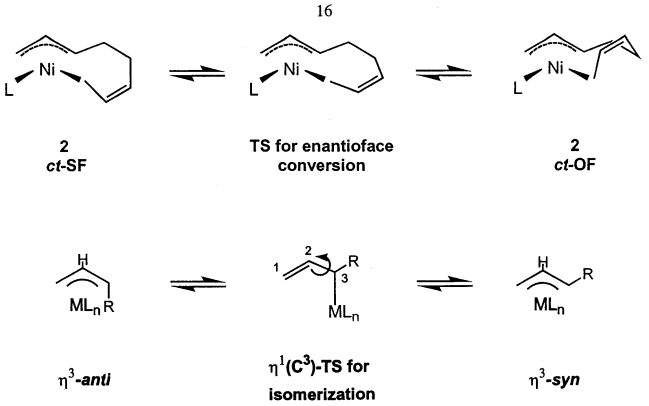

Figure 4. Allylic enantioface conversion in **2** (top) and allylic isomerization in **3** taking place via an η^1(C^3)-allylic intermediate (below).

η^3,η^1(C^1) configuration **2**, while in the case of the weak σ-donor PPh_3, as well as the π-acceptor $P(OPh)_3$, **4** is predicted to have the highest thermodynamic population.

C. Allylic Syn−Anti Isomerization and Allylic Enantioface Conversion. The interconversion of the syn and anti configuration of the terminal allylic groups in the [(octadienediyl)Ni^{II}L] complex as well as the allylic enantioface conversion represent crucial steps in the overall cyclodimerization process, since different stereoisomers are involved along the most feasible pathways for oxidative coupling and reductive elimination; thus, these processes operate under different stereocontrol. Allylic isomerization most likely takes place via a $\eta^3 \rightarrow \eta^1$(C^3) allylic rearrangement followed by subsequent internal rotation of the vinyl group around the C^2−C^3 single bond, with the η^3,η^1(C^3) species **3** acting as precursor. Conversion of the allyl group's enantioface preferably proceeds in the η^3,η^1(C^1) species **2** by interconverting the η^1-allylic group (cf. Figure 4). Butadiene is unlikely to participate in these two processes, as shown in our previous study.[7] The absolute barriers ($\Delta G^{\ddagger}$) of allylic isomerization and enantioface conversion (Tables S2 and S3) fall within a narrow range and differ by less than 1 kcal mol^{-1} for individual catalysts. For enantioface conversion, an activation free energy ($\Delta G^{\ddagger}$) of ∼10.5 kcal mol^{-1} has to be overcome, while the overall highest free energy barrier ($\Delta G^{\ddagger}$) for allylic isomerization amounts to ∼18.7 kcal mol^{-1}. These two processes clearly represent the most feasible ones among all elementary steps in the catalytic cycle involving the [(octadienediyl)Ni^{II}L] complex. Accordingly, the equilibrium between different species of the [(octadienediyl)Ni^{II}L] complex and their several stereoisomeric forms can likely be supposed as always being attained.

D. Reductive Elimination under Ring Closure. The principal cyclodimer products are generated along competing routes for reductive elimination, starting from either the square-planar η^3,η^1(C^1) species **2** or the square-pyramidal bis-η^3 species **4** of the [(octadienediyl)Ni^{II}L] complex and giving rise to the trigonal-planar [(η^4-cyclodimer)Ni^{0}L] products **8**−**10**. VCH is formed along **2** → **8**, and the generation of both *cis*-1,2-DVCB and *cis*,*cis*-COD starts from the precursor **4** along the **4** → **9** and **4** → **10** routes, respectively.

D.1. Formation of VCH. Formation of VCH along **2** → **8** preferably takes place via the pathway that involves the *cc*-SF coupling stereoisomer (Table S4). The six-membered ring is generated by formation of a C−C σ-bond between the η^3-allylic-C^3 and the terminal η^1-allylic-C^8 in the square-planar product-like TS[**2**−**8**]. As revealed by Figure 5, TS[**2**−**8**] is very similar for all catalysts[28] and occurs at a distance of ∼2.01−2.03 Å of the new bond being formed. Overall, similar to the findings for the generic catalyst,[7] reductive elimination affording VCH represents that process of the catalytic cycle that is the least influenced by the different kind of butadiene coupling, as indicated by similar activation barriers and reaction energies for several stereoisomeric pathways (cf. Table S4).

Table 3 displays the energetics for the most feasible *cc*-SF stereochemical pathway together with the estimated contributions of the electronic and steric factors, which both follow a quite regular trend. Electron-donating ligands raise the intrinsic activation energy uniformly by ∼1 kcal mol^{-1}, when compared with the generic catalyst. On the other hand, π-acceptor ligands tend to stabilize TS[**2**−**8**] relative to **2**, giving rise to a reduction of the activation barrier that correlates inversely with the ligand's acceptor strength. Thus, the kinetic barrier, as regards the electronic influence, is indicated to be mainly determined by the ligand's π-acceptor ability. This can be rationalized by simple molecular orbital arguments. Reductive elimination is accompanied with a formal electron redistribution between the [NiL] and [C_8H_{12}] moieties, giving rise to a reduction of the oxidation number on nickel by two, namely Ni^{II} → Ni^0. A low-lying acceptor d-orbital on nickel, which is able to mix

(28) We focus here essentially on the octadienediyl framework, although the Ni−L distance changes due to the different electronic and steric properties of the individual PMe_3, PPh_3, $P(^iPr)_3$, and $P(OPh)_3$ ligands.

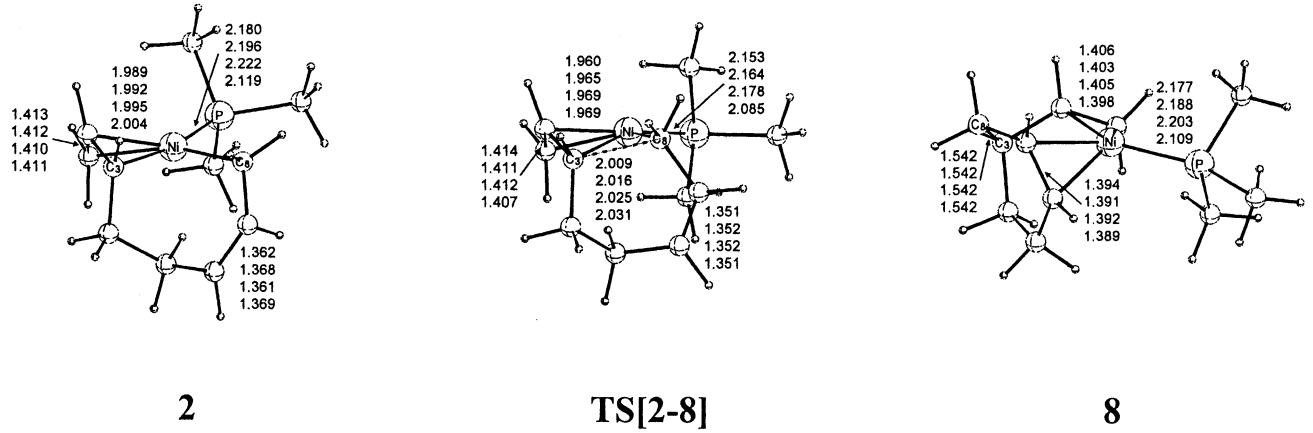

Figure 5. Selected geometric parameters (Å) of the optimized structures of key species for reductive elimination affording VCH for the [(octadienediyl)-Ni^{II}L] complex via the most feasible *cc*-SF stereochemical pathway along **2** → **8**. See Figure 2.

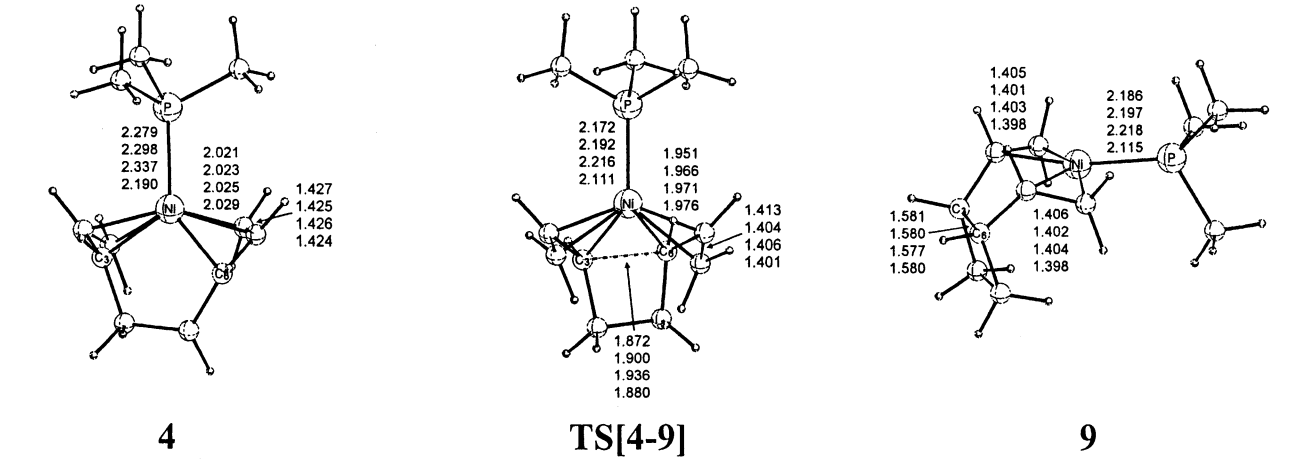

Figure 6. Selected geometric parameters (Å) of the optimized structures of key species for reductive elimination affording *cis*-1,2-DVCB for the [(octadienediyl)-Ni^{II}L] complex via the feasible *cc*-OF stereochemical pathway along **4** → **9**. See Figure 2.

efficiently into the octadienediyl 2π-orbital, facilitates the process kinetically by stabilizing the transition state. Acceptor ligands decrease the energetic gap between these two orbitals and therefore accelerate the reductive elimination by reducing the activation barrier. Steric pressure on the ligand is seen to lower the activation energy as well, since this process goes along with a formal reduction of the coordination number on nickel from 4 to 3 along **2** → **8**. This implies a relief of the steric pressure caused by bulky ligands, as indicated by the reduction of the Ni—L distance (cf. Figure 5). Moderate steric bulk [L = PMe_3, PPh_3, $P(OMe)_3$] has a minor influence and for this case the barrier is predicted to be mainly determined by electronic factors. With increase of the steric pressure, the steric effect becomes prevalent, which is most remarkable for the bulky, space-demanding $P(^tBu)_3$.

Overall, the lowest intrinsic free energy barrier of 20.5 kcal mol^{-1} ($\Delta G_{int}^{\ddagger}$) is calculated for **IV** (L = $P(OPh)_3$), where both electronic and steric factors are found to assist the VCH formation to a similar amount. Higher intrinsic activation barriers ($\Delta G_{int}^{\ddagger}$) have to be overcome for catalysts bearing moderately bulky donor phosphines, 23.7 and 23.3 kcal mol^{-1} for **I** and **II** (L = PMe_3, PPh_3), respectively, due to the limited π-acceptor ability of these ligands. The destabilization of the transition state caused by electronic effects is, however, compensated by introducing steric bulk on the ligand. The barrier is thus reduced to 21.8 kcal mol^{-1} ($\Delta G_{int}^{\ddagger}$) for **III** bearing the bulky donor $P(^iPr)_3$.

Reductive elimination along **2** → **8** leads to the thermodynamically most stable product **8** among all of the [(η^4-cyclodimer)Ni^{0}L] complexes **8**−**10**, in a process that is exogonic by ∼11.2−14.2 kcal mol^{-1} (ΔG_{int}). Similar to the trends obtained for the kinetic barrier, VCH generation is found to be favored thermodynamically by the increase of the ligand's π-acceptor ability. Thus [VCH] → [NiL] donation seems to be the dominant electronic effect for stabilizing of **8**, along with the support due to steric pressure on the ligand.

D.2. Formation of *cis*-1,2-DVCB and *cis,cis*-COD. *cis*-1,2-DVCB and *cis,cis*-COD are generated along the **4** → **9** and **4** → **10** routes, respectively, by establishing a σ-bond between either the substituted terminal carbons (C^3, C^6 Figure 6) or the unsubstituted terminal carbons (C^1, C^8 Figure 7) of the two η^3-allylic groups in **4**. Both, *cis*-1,2-DVCB and *cis,cis*-COD are the kinetically preferred products along these routes, since the formation of other isomers is precluded by higher activation barriers (Tables S5 and S6).[29] Very similar activation barriers have to be overcome for *cis*-1,2-DVCB generation with the bis-(η^3-anti) *cc*-OF coupling stereoisomer and the η^3-anti/syn *ct*-

(29) We have focused on the *cis*/*cis*-butadiene OF stereoisomeric pathway in the investigation of the *cis,cis*-COD generating **4** → **10** route, which has been shown to be distinctly preferred by both thermodynamic and kinetic reasons for the generic [bis(η^2-butadiene)Ni^{0}PH$_3$] catalyst (ref 7).

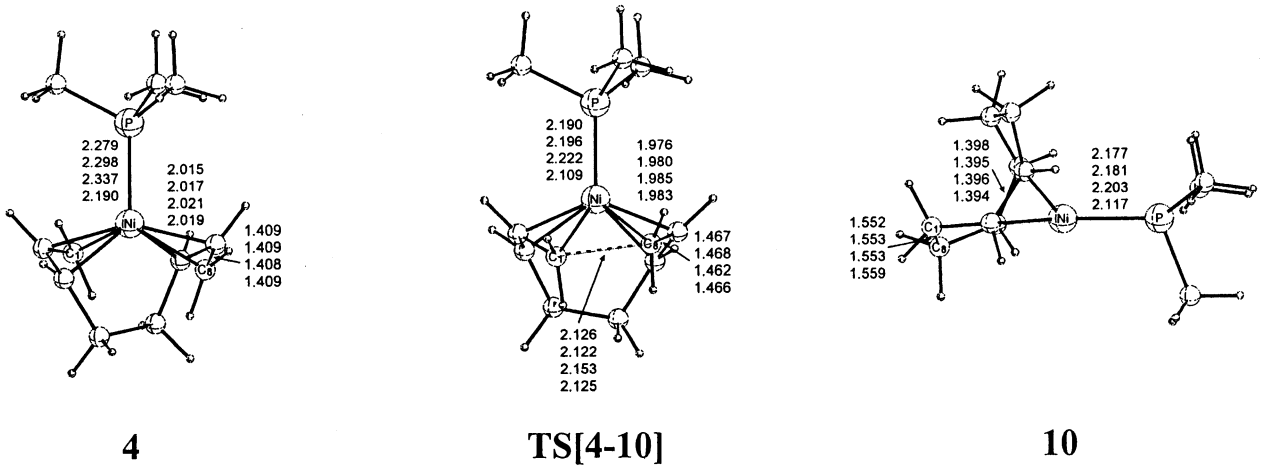

Figure 7. Selected geometric parameters (Å) of the optimized structures of key species for reductive elimination affording *cis*,*cis*-COD for the [(octadienediyl)-$Ni^{II}L$] complex via the most feasible *cc*-OF stereochemical pathway along **4** → **10**. See Figure 2.

Table 4. Intrinsic Activation Enthalpies and Free Energies ($\Delta H_{Int}^{\ddagger}/\Delta G_{Int}^{\ddagger}$ in kcal mol^{-1}) and Reaction Enthalpies and Free Energies ($\Delta H_{Int}/\Delta G_{Int}$ in kcal mol^{-1}) for Reductive Elimination Affording *cis*-1,2-DVCB for the [(Octadienediyl)$Ni^{II}L$] Complex via the Feasible *cc*-OF Stereochemical Pathway along **4** → **9**, Together with an Estimate of Electronic and Steric Contributions to Relative Activation Barriers and Reaction Energies ($\Delta\Delta E^{\ddagger}$, $\Delta\Delta E$ in kcal mol^{-1})[a-c]

	L = PH_3	**I**, L = PMe_3	**II**, L = PPh_3	**III**, L = $P(^iPr)_3$	**IV**, L = $P(OPh)_3$	**V**, L = $P(OMe)_3$	**VI**, L = $P(^tBu)_3$
$\Delta H_{QM}^{\ddagger}/\Delta G_{QM}^{\ddagger}$	15.27/16.12	13.83/14.47	13.57/14.22	12.44/13.08	12.73/13.25		
$\Delta H_{QM}/\Delta G_{QM}$	−6.14/−5.47	−8.69/−7.86	−6.21/−5.37	−10.12/−9.28	−6.31/−5.83		
$\Delta E_{QM}^{\ddagger}$	16.11	14.75	14.49	13.36	13.75	14.22	12.36
$\Delta E_{QM/MM}^{\ddagger}$		16.09	15.64	14.56	15.59	16.06	13.63
$\Delta\Delta E^{\ddagger}$ [b]		−1.36	−1.62	−2.75	−2.36	−1.89	−3.75
$\Delta\Delta E_{el}^{\ddagger}/\Delta\Delta E_{st}^{\ddagger}$		−1.34/−0.02	−1.15/−0.47	−1.20/−1.55	−1.84/−0.52	−1.75/−0.04	−1.27/−2.48
ΔE_{QM}	−6.34	−9.09	−6.61	−10.52	−6.55	−6.50	−9.67
$\Delta E_{QM/MM}$		−6.37	−6.36	−7.58	−6.43	−6.40	−8.02
$\Delta\Delta E$[c]		−2.75	−0.27	−4.18	−0.21	−0.16	−3.33
$\Delta\Delta E_{el}/\Delta\Delta E_{st}$		−2.72/−0.03	−0.25/−0.02	−2.94/−1.24	−0.12/−0.09	−0.10/−0.06	−1.65/−1.68

[a] Intrinsic barriers and reaction energies relative to the [(bis(η^3-*anti*)-octadienediyl)$Ni^{II}L$] *cc*-OF isomer of **4**. The values for the generic catalyst taken from our previous study[7] are included for comparison. [b,c] See Table 1.

SF coupling stereoisomer of **4** involved. Although the latter pathway is kinetically slightly preferred, the product **9** rearranges into the thermodynamically more stable *cis*-1,2-DVCB isomer arising from the *cc*-SF stereochemical pathway. Formation of *cis*,*cis*-COD preferably proceeds commencing from the bis(η^3-anti) *cc*-OF coupling stereoisomer of **4**, due to both kinetic and thermodynamic reasons (Tables S5 and S6).[29] Similar to the findings for the VCH formation pathway, the geometry of the octadienediyl framework in TS[**4**−**9**] and TS[**4**−**10**], respectively, is seen to be very similar for all catalysts investigated (Figures 6 and 7).[28] The cyclodimers are found to be essentially preformed in TS[**4**−**9**] and TS[**4**−**10**]. The transition states thus appear being product-like, occurring at a distance of ∼1.87−1.94 and ∼2.12−2.15 Å, respectively, for the new C−C bond being formed.

We shall analyze the influence of the ligand on the kinetics of the **4** → **9** and **4** → **10** routes for the *cc*-OF stereochemical pathway (cf. Tables 4 and 5). It follows from these tables that the reductive elimination affording *cis*-1,2-DVCB and *cis*,*cis*-COD is affected quite similarly by electronic and steric factors, with the two effects following a regular trend. Similar to the VCH-generating pathway discussed in the previous section, the intrinsic barriers are shown to be determined predominantly by the π-acceptor ability of the ligand, as far as the electronic effect is concerned. Electron-donating ligands are found to lower the activation energy uniformly by ∼0.8 kcal mol^{-1} relative to the generic catalyst. The process is facilitated by increasing the ligand's π-acceptor strength, since the barriers are predicted to be reduced further for **IV** and **V**, following the order $P(OPh)_3$ > $P(OMe)_3$. On the other hand, bulky ligands act to stabilize the transition states and thus support the reductive elimination.

Reductive elimination affording *cis*-1,2-DVCB and *cis*,*cis*-COD is accompanied by very similar intrinsic activation barriers ($\Delta G_{int}^{\ddagger}$) for all the catalysts. The overall lowest and very similar intrinsic barriers for **III** (L = $P(^iPr)_3$) and **IV** (L = $P(OPh)_3$) ($\Delta\Delta G_{int}^{\ddagger}$ ∼0.2 kcal mol^{-1}) are determined by different factors. For **III** the moderate barrier is due to a stabilization of the transition state relative to bis(η^3-anti) precursor **4**, as a result of reduced steric interactions. In contrast, for **IV** the π-acceptor ability of $P(OPh)_3$ is clearly decisive for the relative stabilization of the transition state, with sterics playing a minor role. Higher intrinsic activation energies ($\Delta G_{int}^{\ddagger}$) have to be overcome for **I** and **II** (L = PMe_3, PPh_3, respectively), since sterics here has a minor influence on the barrier.

In contrast to the very similar kinetics for *cis*-1,2-DVCB and *cis*,*cis*-COD formation for a given catalyst, the thermodynamics is quite different. *cis*,*cis*-COD is clearly seen as the thermodynamic preferred cyclodimer, while *cis*-1,2-DVCB formation is calculated to be less exogonic (ΔG) for all catalysts. The difference in stability between the [(η^4-cyclodimer)Ni^0L] products **9** and **10** is most remarkable for **IV** (L = $P(OPh)_3$) and

Table 5. Intrinsic Activation Enthalpies and Free Energies ($\Delta H_{int}^{\ddagger}/\Delta G_{int}^{\ddagger}$ in kcal mol^{-1}) and Reaction Enthalpies and Free Energies ($\Delta H_{int}/\Delta G_{int}$ in kcal mol^{-1}) for Reductive Elimination Affording *cis*,*cis*-COD for the [(Octadienediyl)Ni^{II}L] Complex via the Most Feasible *cc*-OF Stereochemical Pathway along **4** → **10**, Together with an Estimate of Electronic and Steric Contributions to Relative Activation Barriers and Reaction Energies ($\Delta\Delta E^{\ddagger}$, $\Delta\Delta E$ in kcal mol^{-1})[a-c]

	L = PH_3	**I**, L = PMe_3	**II**, L = PPh_3	**III**, L = $P(^iPr)_3$	**IV**, L = $P(OPh)_3$	**V**, L = $P(OMe)_3$	**VI**, L = $P(^tBu)_3$
$\Delta H_{QM}^{\ddagger}/\Delta G_{QM}^{\ddagger}$	13.34/14.81	12.41/13.68	12.48/13.75	11.09/12.36	11.43/12.56		
$\Delta H_{QM}/\Delta G_{QM}$	−8.90/−7.93	−10.34/−9.86	−10.87/−10.38	−13.48/−12.99	−12.87/−12.53		
$\Delta E_{QM}^{\ddagger}$	13.62	12.78	12.85	11.46	11.87	12.11	10.08
$\Delta E_{QM/MM}^{\ddagger}$		13.63	13.50	12.19	13.71	13.64	11.01
$\Delta\Delta E^{\ddagger}$ [b]		−0.84	−0.77	−2.16	−1.75	−1.51	−3.45
$\Delta\Delta E_{el}^{\ddagger}/\Delta\Delta E_{st}^{\ddagger}$		−0.85/0.01	−0.65/−0.12	−0.73/−1.43	−1.84/0.09	−1.53/0.02	−0.93/−2.61
ΔE_{QM}	−10.02	−11.43	−11.96	−14.57	−13.82	−12.49	−18.45
$\Delta E_{QM/MM}$		−10.04	−10.14	−11.51	−11.01	−10.08	−15.93
$\Delta\Delta E$[c]		−1.41	−1.82	−4.55	−3.80	−2.47	−8.43
$\Delta\Delta E_{el}/\Delta\Delta E_{st}$		−1.39/−0.02	−1.94/−0.12	−3.06/−1.42	−2.81/−0.99	−2.41/−0.06	−2.52/−5.91

[a] Intrinsic barriers and reaction energies relative to the [(bis(η^3-*anti*)-octadienediyl)Ni^{II}L] *cc*-OF isomer of **4**. The values for the generic catalyst taken from our previous study[7] are included for comparison. [b,c] See Table 1.

amounts to 6.7 kcal mol^{-1} ($\Delta\Delta G$). We shall elaborate further on the implications for the regulation of the product selectivity in the next section.

II. Regulation of the Cyclodimer Product Selectivity. The role of electronic and steric factors have been elucidated for all crucial elementary steps of the entire catalytic cycle in the preceding sections. The mechanistic conclusions drawn in our previous investigation of the generic catalyst[7] were corroborated in the present examination of the real catalysts **I**−**IV**. Among the different stereochemical pathways possible for each individual elementary process, we found that the preferred pathway for a given process was the same for all catalysts. Furthermore, these favored stereochemical pathways are identical to those predicted for the generic catalyst.[7] The [(octadienediyl)Ni^{II}L] complex is generated via oxidative coupling of two η^2-butadienes along **1** → **2**, which is seen to be influenced to a minor extent by electronic and steric factors. The different configurations of the [(octadienediyl)Ni^{II}L] complex, with **2** and **4** being the prevailing species, and their several stereoisomeric forms are in a kinetically mobile preestablished equilibrium that can be regarded as always being present. For reductive elimination the overall largest kinetic barriers of the entire catalytic cycle have to be overcome; thus, these steps are predicted to be rate-determining.

For this typical Curtin−Hammett situation,[30] the selectivity of the cyclodimer production, therefore, is entirely determined kinetically by the ratio of the absolute kinetic barriers ($\Delta\Delta G^{\ddagger}$) for the three competing routes affording the principal cyclodimers VCH, *cis*-1,2-DVCB, and *cis*,*cis*-COD along **2** → **8**, **4** → **9**, and **4** → **10**, respectively. Two aspects are important for elucidating the ligand's influence on the regulation of the product selectivity. On one hand, the catalytic activity as well as the selectivity are regulated by the concentration of the active precursor species **2** and **4**, which is determined by the position of the preestablished equilibrium between these two species. This represents the thermodynamic-related aspect. The thermodynamic population of different [(octadienediyl)Ni^{II}L] species is indicated to be mainly determined by electronic factors, with sterics playing a minor role (section B). For π-acceptor ligands as well as weak σ-donors, **4** is the prevailing species, while the **2** ⇌ **4** equilibrium becomes displaced to the left upon increasing of the ligand's σ-donor strength. The [(octadienediyl)Ni^{II}L] complex exists predominantly in the $\eta^3,\eta^1(C^1)$ configuration **2** for strong σ-donors. On the other hand, the intrinsic reactivity of **2** and **4** is of crucial importance for the regulation of the product selectivity. The reductive elimination is shown to be facilitated kinetically by the increase of the ligand's π-acceptor ability as well as by bulky, space-demanding ligands. In the absence of high steric pressure, the electronic influence is prevalent, while for ligands that are sterically bulky the steric factor becomes dominant. The three competing routes for reductive elimination, however, are not influenced in a uniform way by electronic and steric factors. The **2** → **8** VCH formation route is seen to be influenced by both factors to a larger extent, relative to the **4** → **9**/**10** routes affording *cis*-1,2-DVCB and *cis*,*cis*-COD, respectively.

As outlined in the outset, a careful experimental investigation of the influence of the ligand on the cyclodimer product distribution was undertaken by Heimbach et al.[5] Strong π-acceptor ligands that are sufficiently space-demanding were found to catalyze the formation of *cis*,*cis*-COD almost exclusively. The VCH portion at first becomes enlarged with the increase in the ligand's σ-donor strength, passing through a maximum with a *cis*,*cis*-COD:VCH product ratio of ∼50:50 and decreasing afterward for strong σ-donor ligands, with *cis*,*cis*-COD becoming prevalent. From their statistical analysis Heimbach et al.[5] concluded that electronic factors are entirely decisive for the cyclodimer product distribution and sterics overall have no pronounced influence.

Table 6 collects the absolute activation free energies ($\Delta G^{\ddagger}$) for the three competing reductive elimination routes, with **2** chosen as an arbitrary reference, together with the difference between the barriers ($\Delta\Delta G^{\ddagger}$) for the two major cyclodimer products, VCH and *cis*,*cis*-COD (vide infra). The order of the absolute barriers for the VCH-generating route for catalysts **I**−**IV** follows that predicted for the intrinsic barriers (section D.1). The same holds true for the **4** → **9**/**10** routes that afford *cis*-1,2-DVCB and *cis*,*cis*-COD, respectively, by taking the difference in the thermodynamic stability between **2** and **4** into account. For all catalysts very similar barriers are predicted for generation of *cis*-1,2-DVCB and *cis*,*cis*-COD. The reverse oxidative addition under C−C cleavage, however, is indicated to be more facile along **9** → **4** when compared to **10** → **4**, since **9** is distinctly less stable, thermodynamically, than **10** (section D.2). This would indicate that *cis*,*cis*-COD is formed as the principal product along the routes that starts from the bis-η^3

(30) (a) Seemann, J. I. *Chem. Rev.* **1983**, *83*, 83. (b) Seemann, J. I. *J. Chem. Educ.* **1986**, *63*, 42.

Table 6. Absolute Activation Enthalpies and Free Energies ($\Delta H^{\ddagger}/\Delta G^{\ddagger}$ in kcal mol^{-1}) for Reductive Elimination Affording VCH, *cis*-1,2-DVCB, and *cis*,*cis*-COD for the [(Octadienediyl)Ni^{II}L] Complex via the Most Feasible Individual Stereochemical Pathway along **2** → **8**, **4** → **9**, and **4** → **10**, Respectively[a,b]

	$\Delta H^{\ddagger}/\Delta G^{\ddagger}$			
	I, L = PMe_3	**II**, L = PPh_3	**III**, L = $P(^iPr)_3$	**IV**, L = $P(OPh)_3$
VCH *cc*-SF **2** → **8**	24.7/24.8	23.6/23.7	23.0/23.1	21.4/21.2
cis-1,2-DVCB *ct*-SF **4** → **9**	22.8/23.4	20.0/20.6	21.8/22.4	18.7/19.2
cis,*cis*-COD *cc*-OF **4** → **10**	23.1/24.1	19.9/20.9	21.8/22.8	17.9/19.0
$\Delta\Delta G^{\ddagger}$ [b] VCH/*cis*/*cis*-COD	0.7	2.8	0.3	2.2

[a] Absolute barriers relative to the [(η^3-*syn*,η^1(C^1),Δ-*cis*-octadienediyl)-Ni^{II}L] *ct*-OF isomer of **2**. [b] Difference in the absolute activation free energies between the competing routes for generation of the two major cyclodimer products, VCH and *cis*,*cis*-COD; the positive sign indicates a lower barrier for *cis*,*cis*-COD formation, relative to that for VCH formation.

species **4**, since the thermodynamically instable *cis*-1,2-DVCB would be transformed under thermodynamic control into *cis*,*cis*-COD along **9** → **4** → **10**. This is consistent with the experimental observation for catalysts with a weak σ-donor or an π-acceptor ligand, which likely catalyze the cyclodimer formation via the routes involving **4**. For these catalysts *cis*-1,2-DVCB can be isolated as an intermediate product in up to 40% yield together with *cis*,*cis*-COD, which is understandable from the very similar barriers predicted for the two processes, while VCH is not formed.[10a,31,32] After all the butadiene has been consumed the amount of *cis*-1,2-DVCB in the product mixture decreases, and after a certain period the *cis*-1,2-DVCB is transformed completely into the thermodynamically more stable *cis*,*cis*-COD.[10a]

In agreement with experiment,[2c,5b,c,32] catalysts **II** and **IV** bearing the weak σ-donor PPh_3 and the π-acceptor $P(OPh)_3$, respectively, are predicted to predominantly catalyze the formation of *cis*,*cis*-COD ($\Delta\Delta G^{\ddagger}$ = 2.8 and 2.2 kcal mol^{-1}, respectively, with **4** → **10** in favor relative to **2** → **8**). The calculated $\Delta\Delta G^{\ddagger}$ value of 2.8 kcal mol^{-1} for **II** is certainly overestimated, since **2** is likely to be populated to a certain extent for weak σ-donors, which would give rise to a moderate VCH portion of ∼25%.[2c,5b,c,32] For **IV**, *cis*,*cis*-COD should almost exclusively be formed, while the **2** → **8** route affording VCH is likely to be essentially suppressed. The **4** → **10** route is favored by both thermodynamic and kinetic reasons, since π-acceptor ligands are shown to displace the preestablished **2** ⇌ **4** equilibrium strongly far to the right (section B), and thus give rise to a high concentration of the precursor **4**, and also to reduce the kinetic barrier (section D.2.). Consequently, the increase in the *cis*,*cis*-COD selectivity is accompanied by an increase of the catalytic reactivity.[2c,32] The activity and selectivity of *cis*,*cis*-COD formation can be enhanced further by π-acceptor ligands that are sterically bulky (section D.2), due to kinetic reasons (further reduction of the activation barrier) and to a lesser extent also by thermodynamic reasons (increase of the thermodynamic population of **4**). This is consistent with the experimental observation that the highest reaction rate and the highest yield of *cis*,*cis*-COD is obtained for the bulky $P(OC_6H_4$-*o*-$Ph)_3$ ligand (96%).[2c,5b,c,32,33]

The present study indicates that the barriers for reductive elimination become higher with increase of the ligand's σ-donor strength. The route for VCH generation is likely to be retarded to a larger extent than the route for *cis*,*cis*-COD formation (sections D.1,2). This, however, is compensated for by the displacement of the preestablished equilibrium to the left, which increases the concentration of the precursor species **2**. Consequently, the VCH portion becomes enlarged up to a certain extent, together with a decrease in the catalytic activity. Both aspects are consistent with experiment.[5b,c] From our present analysis, we believe that the subtle balance between these two effects must be considered responsible for the fact that the maximal yield of VCH never exceeds 55%.[2c,5b,c,32]

For catalysts **I** and **III** with the stronger σ-donors PMe_3 and $P(^iPr)_3$, the calculated relative absolute barriers for the *cis*,*cis*-COD and VCH formation ($\Delta\Delta G^{\ddagger}$) of 0.7 and 0.3 kcal mol^{-1}, respectively, indicates that the *cis*,*cis*-COD portion becomes reduced to approximately 50%, which is in excellent agreement with experiment.[2c,5b,c,34]

Concluding Remarks

We have presented a comprehensive theoretical investigation of the influence of ligand L on the regulation of the selectivity for the [Ni^{0}L]-catalyzed cyclodimerization of 1,3-butadiene based on DFT and a combined DFT/MM (QM/MM) method. This reaction represents that process in homogeneous catalysis where "ligand tailoring" was discovered for the first time and has been explored to the greatest detail. However, a comprehensive understanding of the ligand's influence on individual elementary steps has still been lacking. This gap is filled by our theoretical study, where the role of electronic and steric effects has been elucidated for all crucial elementary steps of the whole catalytic cycle for the real [bis(butadiene)Ni^{0}L] catalyst complexes with L = PMe_3, **I**; L = PPh_3, **II**; L = $P(^iPr)_3$, **III**; and L = $P(OPh)_3$, **IV**. On the basis of this analysis a theoretically well-founded, detailed understanding of both the thermodynamic and the kinetic aspects of the regulation of the product selectivity in the [Ni^{0}L]-catalyzed cyclodimerization of 1,3-butadiene is provided. To the best of our knowledge, the present theoretical investigation represents one of the very few examples where it has been possible to elucidate in a detailed manner the role of electronic and steric factors for individual elementary steps on the basis of quantum chemical calculations.

The catalytic cycle suggested in our previous investigation on the generic catalyst (L = PH_3),[7] which was based on an original proposal by Wilke et al.,[2,8] has been corroborated in all details. The [(octadienediyl)Ni^{II}L] complex is formed by oxidative coupling of two η^2-butadienes along **1** → **2**. A kinetically mobile preestablished equilibrium can be assumed for the different configurations of this complex, with **2** and **4** as the prevailing species, in their various stereoisomeric forms. The principal cyclodimer products are formed along competing routes for reductive elimination, which is predicted to be rate-limiting.

(31) Heimbach, P.; Jolly, P. W.; Wilke, G. *Adv. Organomet. Chem.* **1970**, *8*, 29.
(32) Brenner, W.; Heimbach, P.; Hey, H.; Müller, E. W.; Wilke, G. *Justus Liebigs Ann. Chem.* **1967**, *727*, 161.

(33) We have estimated the experimental free energy of activation for the bulky π-acceptor $P(OC_6H_4$-*o*-$Ph)_3$, which almost exclusively catalyzes the formation of *cis*,*cis*-COD (96% selectivity), by the following crude approximation: With a TOF of 780 g BD (g Ni)$^{-1}$ h^{-1} at 353 K,[2c] one obtains an effective rate constant $k \sim 0.23$ s^{-1} and $\Delta G^{\ddagger} \sim 21.8$ kcal mol^{-1}, by applying the Eyring equation with $k = 2.08\ 10^{10} T \exp(-\Delta G^{\ddagger}/RT)$. This value agrees very well with the calculated barrier of 20.1 kcal mol^{-1} ($\Delta G^{\ddagger}$) for catalyst **IV** [L = $P(OPh)_3$] for the rate-determining reductive elimination along **4** → **10**, relative to the overall most stable species of the catalytic cycle, namely the *tt*-OF bis(η^3-syn) species **4**.
(34) A *cis*,*cis*-COD yield of 56−57% was observed for catalysts with the strong donors PEt_3 and $P(^iPr)_3$.[5b,c] Catalyst **I** (L = PMe_3) can be considered as a good model for the experimentally examined catalyst with L = PEt_3.

The energetics calculated for allylic syn−anti isomerization via **2**, allylic enantioface conversion in **3**, and also for oxidative coupling along **1** → **2** are very similar for individual catalysts. These elementary processes thus appear to be less influenced by electronic and steric factors. In contrast, the ligand's nature has a pronounced effect on both the equilibrium between **2** and **4** as well as on reductive elimination. Electronic factors are shown to determine the position of the **2** ⇌ **4** equilibrium to a substantial extent. For π-acceptor ligands (L = $P(OPh)_3$) as well as for weak σ-donors (L = PPh_3), **4** is the prevalent species. The increase of the ligand's donor strength displaces the **2** ⇌ **4** equilibrium to the left, and for stronger σ-donors (L = PMe_3, $P(^iPr)_3$), **2** is predominant. The π-acceptor ability as well as the steric bulk on the ligand act to accelerate the reductive elimination by stabilizing the transition states. The barrier height is found to correlate inversely with the two effects. In the absence of serious steric pressure, the barrier is essentially determined by electronic effects, while for ligands that are bulky, the steric factor becomes dominant.

Two processes are shown to be of crucial importance for elucidating the regulation of the selectivity of the cyclodimerization process, namely, the equilibrium between **2** and **4** and the reductive elimination along competing routes. The rationalization of the ligand's role for the thermodynamics and kinetics of these processes provides a deep, fundamental understanding of the selectivity control in the [Ni^0L]-catalyzed cyclodimerization of 1,3-butadiene.

Catalysts bearing π-acceptor ligands that are sufficiently bulky (such as **IV**, L = $P(OPh)_3$) are predicted to catalyze almost exclusively the formation of *cis*,*cis*-COD along **4** → **10**. The same route is passed through by catalysts with weak σ-donors (such as **II**, L = PPh_3), although in this case the VCH generation route along **2** → **8** is not completely suppressed, since **2** is populated to a certain extent. For reductive elimination following the routes that involves **4**, *cis*,*cis*-COD is predicted as the exclusive product, since the intermediate, less stable *cis*-1,2-DVCB is likely to rearrange under thermodynamic control into the more stable *cis*,*cis*-COD. Both aspects agree with the experimental observation.[2c,5b,c,10a,32] For catalysts with ligands that are π-acceptors the route for formation of *cis*,*cis*-COD is favored by both thermodynamic (due to the high concentration of the precursor **4**, by displacing the **2** ⇌ **4** equilibrium to the right) and kinetic reasons (lowering of the activation barrier), relative to the competing route for VCH formation that involves **2**. This route should essentially be suppressed in this case. Furthermore, the correlation observed by experiment[2c,32] between *cis*,*cis*-COD selectivity and catalytic reactivity has its origin in the thermodynamic and kinetic aspects. In agreement with experiment, severe steric bulk is shown to act to enlarge the catalytic activity as well as the *cis*,*cis*-COD selectivity further.

The barriers for reductive elimination are shown to rise upon increasing the ligand's σ-donor strength, but not uniformly. The **2** → **8** route is likely to be retarded to a larger extent than the **4** → **10** route, which, however, is compensated for by the higher concentration of **2**, due to the shift of the **2** ⇌ **4** equilibrium to the left. Accordingly, the VCH portion gets increased up to a certain extent, which is accompanied by a decrease of the catalytic activity. Both aspects are in agreement with experiment.[5b,c] For **I** (L = PMe_3) and **III** (L = $P(^iPr)_3$) the estimated VCH:*cis*,*cis*-COD ratio agrees well with experiment.

Acknowledgment. S.T. is grateful to Prof. Dr. Rudolf Taube for his ongoing interest in this research, which serves as a continuous source of stimulation. S.T. is furthermore indebted to Prof. Dr. R. Ahlrichs (University of Karlsruhe, Germany) for making the latest version of TURBOMOLE available. Excellent service by the computer centers URZ Magdeburg and URZ Halle is gratefully acknowledged. I thank the Deutsche Forschungsgemeinschaft (DFG) for financial support by an Habilitandenstipendium.

Supporting Information Available: Full descriptions of the geometries of all species. Also included is the complete collection of the results for different stereochemical pathways for each of the elementary steps of the entire catalytic cycle (Tables S1−S6) (PDF). This material is available free of charge via the Internet at http://pubs.acs.org.

JA020423W